IJE TRANSACTIONS B: Applications Vol. 39, No. 05, (May 2026) 1122-1138

International Journal of Engineering

Journal Homepage: www.ije.ir

Mapping Flood Zone in Khorram Abad River by Integrating Hydrological and Hydraulic Models

E. Fatapour[a], A. Afrous*[b], B. Aminnejad[c], A. Saremi[a], A. Khosrojerdi[a]

[a] Department of Water Science and Engineering, Science and Research Branch, Islamic Azad University, Tehran, Iran
[b] Department of Water Science and Engineering, Dezful Branch, Islamic Azad University, Dezful, Iran
[c] Department of Water Science and Engineering, Rudehen Branch, Islamic Azad University, Rudehen, Tehran, Iran

PAPER INFO

Paper history:
Received 27 January 2025
Received in revised form 08 April 2025
Accepetd 07 May 2025

Keywords:
Floods
WetSpa Model
LISFLOOD-FP Model
River Flow Simulation
Khorram Abad

ABSTRACT

The aim of this study is to investigate the application of an integrated hydrological-hydraulic modeling approach to simulate river flows, flood hydrographs, and flood-prone areas in the Khorram Abad (Iran) drainage basin. In this study, the WetSpa hydrological model and the LISFLOOD-FP hydraulic model were used to simulate river flows and flood zones. Ten years of meteorological data (water years 2005–2006 to 2014–2015) were employed for the simulations. The models were calibrated using data from the first five years, while the subsequent five years of data were used for validation. The WetSpa model was applied to simulate daily flows, and the LISFLOOD-FP model was used to simulate flood-prone areas for different return periods. The WetSpa model successfully simulated daily flows with acceptable accuracy, achieving performance metrics such as the Nash-Sutcliffe Efficiency (NSE) of 0.53 and the Kling-Gupta Efficiency (KGE) of 0.68. For high-flow events, the NSE coefficient reached 0.7, indicating the model's effectiveness in flood prediction. The results from the LISFLOOD-FP model showed that the maximum flood extent for the 200-year return period was 627,100 square meters. The water balance analysis revealed that 25.5% of the precipitation was converted into runoff, comprising 2.34% surface runoff, 1.6% subsurface runoff, and 21.57% groundwater flow. This study demonstrates that the integration of hydrological and hydraulic models can effectively predict flood behavior and delineate high-risk areas.

doi: *10.5829/ije.2026.39.05b.07*

Graphical Abstract

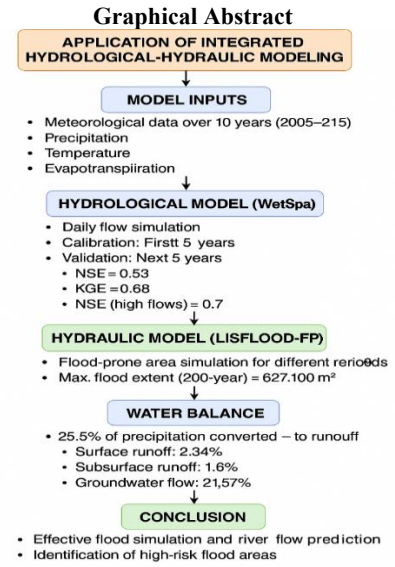

*Corresponding Author Email: Ali.afrous@gmail.com (A. Afrous)

Please cite this article as: Fatapour E, Afrous A, Aminnejad B, Saremi A, Khosrojerdi A. Mapping Flood Zone in Khorram Abad River by Integrating Hydrological and Hydraulic Models. International Journal of Engineering, Transactions B: Applications. 2026;39(05):1122-38.

1. INTRODUCTION

In recent decades, climate change has become one of the most pressing global issues and environmental crises. The far-reaching effects of these changes, observable at both local and global scales, manifest in temperature variations, altered precipitation patterns, and increased climatic instabilities (1). These transformations have led to serious and multifaceted consequences for water resources, food security, ecosystems, infrastructure, and public health (2). Among the most concerning impacts of climate change is the heightened frequency and intensity of extreme weather events, particularly floods and droughts (3). These phenomena pose especially severe threats in countries like Iran, which possesses distinct climatic and geographical characteristics (4). Iran's location within the global arid belt, coupled with its unique topographical features, makes it one of the most vulnerable countries to climate change (5). Decreasing precipitation in many regions, rising temperatures, and the occurrence of sudden heavy rainfall leading to severe flooding exemplify the complex and destructive impacts of these changes. The increasing frequency of large-scale and abrupt floods in recent years underscores the urgent need for comprehensive studies and effective risk management strategies (6).

Flooding, defined as the overflow of water beyond its natural boundaries, often results in widespread damage to agricultural lands, urban infrastructure, financial assets, and human life (7). Floods have been recognized as the most frequent and devastating natural disasters worldwide over the past decade, causing profound environmental, social, and economic consequences (8). Rapid population growth and accelerating industrialization have driven human settlements closer to riverbanks and concentrated economic activities in floodplains. This trend has markedly increased the frequency and severity of flood events (5). In Iran, reports indicate a 40% rise in flood incidents over recent decades (9). Additionally, official statistics reveal that over the past 53 years, more than 12,000 Iranian citizens have lost their lives due to floods. These alarming figures emphasize the critical importance of addressing flood-related issues to mitigate their disastrous impacts (10).

Lorestan Province, due to its distinct hydrological and geomorphological features, is one of the most flood-prone regions in Iran. The combination of narrow riverbeds and the presence of villages and agricultural lands along riverbanks has amplified the financial and human losses caused by floods (5). Over the past 25 years, this province has experienced 30 significant flood events, resulted in the loss of approximately 60 lives during this period (4). These statistics highlight the province's heightened vulnerability and the urgent need for advanced flood risk assessment and management.

Khorramabad River, a crucial watershed in western Iran, plays a vital role in supplying water resources and maintaining the region's ecological balance. In recent decades, this river has experienced severe and unexpected flooding, inflicting extensive damage on agricultural productivity, infrastructure, and water resources (3). Beyond physical destruction, these floods have triggered numerous social and economic challenges, such as forced migrations and escalating poverty in local communities. With ongoing population growth and urban expansion in areas surrounding the river, the region's susceptibility to climate change and flood events has significantly intensified (5). Accordingly, one of the most fundamental approaches to mitigating the destructive impacts of floods is the precise identification of flood-prone areas within watersheds. Floodplains and river-adjacent regions, which serve as hubs for economic and social activities due to their advantageous characteristics, are persistently at risk of flood-related hazards (6). Therefore, in such vulnerable zones, determining the extent of flood inundation, floodwater elevation relative to ground level, and flood characteristics across various return periods commonly known as flood zoning becomes critically important (8).

Despite extensive research on flood mapping and prediction, a significant and well-defined study gap persists regarding the integration of advanced hydrological and hydraulic models with GIS for high-accuracy flood simulation. This gap becomes even more pronounced when considering the complex and multifaceted impacts of climate change. This study explicitly addresses this gap by proposing a comprehensive and innovative approach that combines these techniques for the Khorramabad River watershed. By doing so, this research not only enhances the precision of flood prediction but also establishes a robust framework for future studies in regions with similar climatic and hydrological characteristics. Moreover, this approach offers practical applications for disaster risk reduction and informed urban and environmental planning. The study aims to fill this critical gap by providing a detailed, high-accuracy model that incorporates advanced hydrological and hydraulic modeling techniques integrated with GIS tools.

To date, several methods have been proposed for identifying flood-prone areas, including synoptic flood forecasting (11), flood prediction through river hydrograph analysis (12), and statistical routing and probability-based forecasting of flood occurrence and return periods (13). Hydrological and hydraulic models have proven to be advanced and effective tools for simulating and forecasting various hydrological conditions. These models analyze complex water flow processes, climatic variations, geographical changes, and meteorological data such as rainfall and temperature,

enabling precise predictions of flood timing, magnitude, and location (13). Among these techniques, the integration of Geographic Information Systems (GIS) with hydrological and hydraulic models has opened new frontiers in flood forecasting and simulation (14). GIS-based analyses enable researchers to scrutinize an area's geographical and topographical features in detail and incorporate climate change impacts more accurately into simulation models. This integration not only improves prediction accuracy but also plays a vital role in identifying vulnerable areas susceptible to future flooding (13).

In this study, the selection of hydrological and hydraulic models is meticulously justified based on their demonstrated efficiency, reliability, and adaptability to regions with similar climatic and geographical conditions. The models employed, including advanced rainfall-runoff and water surface elevation simulation techniques, have been extensively validated in previous research and have consistently shown high performance in capturing the unique hydrological dynamics of the Khorramabad River basin. Furthermore, the combination of these models with GIS tools creates a sophisticated and highly accurate framework for detailed flood mapping and comprehensive risk assessment. This integrative approach offers a scientifically robust methodology for addressing the pressing challenges of flood prediction and management, making it the most suitable choice for this research.

The present study, focusing on the Khorramabad River as a representative of sensitive watersheds in Iran, aims to simulate and predict flood occurrences while analyzing the far-reaching impacts of climate change on this basin. For the first time, this research employs an integrated approach that combines advanced hydrological and hydraulic models with GIS-based data analysis. The objective is to develop a comprehensive and highly accurate model for flood prediction and the identification of high-risk areas. Given climate change projections indicating a potential 2°C rise in Iran's temperature by 2030, the significance of this study becomes even more apparent. This anticipated temperature increase, alongside diminishing runoff and escalating drought conditions, is expected to exacerbate the frequency and severity of sudden and intense floods in regions like the Khorramabad basin. Additionally, factors such as rapid population growth, urban sprawl, and vegetation loss further amplify the area's vulnerability, underscoring the urgent need for proactive research and effective flood management strategies.

2. RESEARCH LITERATURE

Rad et al. (10) used the HEC-RAS model in Khorramabad watershed, Iran, to simulate flood profiles and identify flood-prone areas. Their findings showed that significant portions of agricultural and residential land are at risk during floods, emphasizing the need for accurate flood mapping for mitigation planning. Hassas et al. (11) developed a web-based tool for flood spreading modeling using Google Maps DEM data. The tool, applied to the Ayutthaya River flood in Thailand and the Shiraz Flood in 2019, effectively assessed flood risks and aided disaster preparedness planning. Tsegaye et al. (12) integrated GIS with hydrologic-hydraulic modeling to assess flood risks in Bonita Bay, Florida. They have simulated flood inundation due to sea-level rise, land-use changes, and groundwater rise, offering a comprehensive framework for flood risk management.

Chen (13) combined GIS with multi-criteria analysis techniques like AHP and TOPSIS for flood hazard mapping in the Dadu River basin, China. Their approach was successfully identified flood-prone areas, validated by historical flood data. Flores et al. (14) examined flood hazard disparities in Houston, highlighting that minority neighborhoods are disproportionately affected by floods not well-represented in FEMA's maps. The study stressed the need for revised flood risk mapping. Madi et al. (6) integrated the HEC-RAS model into a decision support system for flood prediction in Algeria's Tamanrasset Valley. The study used GIS to assess flood risks under various return periods, demonstrating effective flood zone identification.

Kastridis and Stathis (15) applied the HEC-RAS and SCS models to analyze flash floods in Greece. They found that human activities significantly influenced flood generation, highlighting the importance of land management and GIS-based flood risk analysis. Mudashiru et al. (16) reviewed flood hazard mapping methods, comparing physical, empirical, and modeling techniques. The study emphasized the need for accurate hazard assessment for better flood management strategies. Ahmed et al. (17) used remote sensing, GIS, and AHP techniques to identify flood hazard zones in Tripura, India, showing that AHP is an efficient and cost-effective method for flood risk assessment in data-scarce areas.

El-Bagoury and Gad (18) utilized HEC-HMS and HEC-RAS software for assessing flash flood hazards in two basins in southeastern Cairo, Egypt. By employing meteorological and morphological data and the SCS curve number method, the study calculated discharge volume, peak flow, and flood depth. Runoff volumes for 25-, 50-, and 100-year storms were estimated for An-Nawayah and Al-Rashrash basins. The study identified high, extreme, and medium flood risk zones and proposed constructing dams as a mitigation strategy. Javidan and Bahremand (19) applied the WetSpa model in the Ziyarat basin, Iran, to separate flood flow components. They found that 97% of flood water was base flow during events, providing insights into flood

flow dynamics. El-Saoud and Othman (20) applied GIS and hydrological modeling tools to assess flash flood impacts in the Wadi Mehassar basin near Makkah. Using ArcGIS, ERDAS Imagine, and WMS software, the study processed geological and meteorological data. HEC-1 and HEC-RAS models were utilized to simulate hydrograph curves and inundation extents, identifying 44% of the area as prone to flash flooding. The study highlighted the vulnerability of urban and sacred sites to short-duration, high-intensity rainfall. Cea et al. (21) examined an extreme flood event in Maputo, Mozambique, using high-resolution hydrologic–hydraulic models combined with global data sources. The study validated model outputs with observed data, highlighting the utility of integrated models for flood hazard assessment in data-scarce regions. Results emphasized the role of reservoirs in flood management and the need for enhanced flood risk plans. Hasan et al. (22) investigated urban flash flooding in Aur River catchment, Malaysia, employing XPSWMM software for hydrological and hydraulic simulation. The study used rainfall intensity-duration-frequency data to forecast peak flows and water levels. Results revealed the hydrological changes due to urbanization and emphasized the importance of integrating hydrological analysis in urban flood mitigation planning.

Venkata Rao et al. (23) employed the SWAT and HEC-RAS models to simulate floods in India's Nagavali and Vamsadhara basins. Using 48-hour lead-time rainfall forecasts, the study achieved high accuracy in predicting flood inundation extents and depths. The research highlighted the utility of integrated modeling systems in improving flood preparedness and management during tropical cyclones. Anselmo et al. (24) presented a multi-step integrated modeling approach for flood risk assessment at Montalto di Castro power plant, Italy. The study involved rainfall-runoff modeling, statistical rainfall analysis, and two-dimensional hydraulic modeling. The approach effectively simulated flood events and proved transferable to other flood-prone areas. Ruidas et al. (25) reviewed advancements in flood hazard modeling, focusing on machine learning and metaheuristic techniques. The study evaluated global flood mitigation strategies and highlighted gaps in knowledge regarding regional susceptibility patterns. The research emphasized developing advanced flood prediction models to support early warning systems and flood risk management. Fernández-Nóvoa et al. (26) reviewed global Flood Early Warning Systems (FEWS), focusing on numerical modeling integration. The study discussed the evolution of FEWS from basin-scale applications to global systems, emphasizing their role in mitigating climate-induced flood risks. Key advancements in FEWS development were highlighted as tools for resilience and disaster preparedness. Borga et al. (27) described the Hydrate project's efforts to enhance flash flood forecasting across Europe. The project developed advanced observation strategies and tools for ungauged basins, improving the understanding of flash flood mechanisms. The study underscored the importance of harmonized data and innovative methodologies for effective flash flood risk management. Kumar et al. (28) provided a comprehensive review of flood modeling techniques, including hydrologic, hydraulic, AI-based, and multi-criteria approaches. The study evaluated their effectiveness, challenges, and future prospects, advocating for integrated and advanced models to address data limitations and improve flood risk mitigation strategies.

Al-Omari et al. (29) developed a comprehensive flood hazard map for the King Talal Dam area in Jordan using remote sensing (RS) and GIS methodologies. By integrating key environmental and geographical factors with the Analytic Hierarchy Process (AHP), the study effectively categorized flood risk levels and provided a robust framework for flood risk assessment and disaster management. Yanfatriani et al. (30) analyzed the correlation between extreme weather indices and hydrometeorological disasters in Jambi Province using IMERG rainfall data and disaster records. Their findings revealed significant trends in extreme rainfall and their links to floods, landslides, and droughts, offering valuable insights for regional risk reduction and climate adaptation strategies. Supratman et al. (31) investigated the impact of land use changes on flood hazards in Jakarta's Pondok Karya area by combining Landsat imagery with hydrological and hydraulic modeling tools (HEC-HMS and HEC-RAS). The study highlighted increased flood risk due to urban expansion and vegetation loss, emphasizing the need for effective water management and flood mitigation interventions.

In recent years, numerous studies have focused on flood simulation and prediction, particularly using hydrological and hydraulic models, as well as statistical methods and GIS-based analyses. These studies have explored hydrological processes and flood prediction across various geographic and climatic scales. While many efforts have aimed at achieving more accurate flood simulations and predictions, the use of hydrological and hydraulic models, often in isolation or limited combination with other tools, remains prevalent. This limited integration has led to less accurate predictions and risk assessments in some regions. Given the complexities inherent in hydrological and hydraulic processes, employing advanced models alongside GIS analysis can significantly enhance flood prediction accuracy, improve flood-prone area identification, and optimize water resource management. Additionally, such an approach can lead to more effective crisis planning in vulnerable regions.

Despite significant advances in flood simulation and prediction, the integrated use of hydrological, hydraulic,

and GIS models has not been sufficiently explored in certain regions, particularly in areas with limited data availability. This gap underscores the need for new research that employs more comprehensive approaches to substantially improve prediction accuracy and flood risk management. While numerous studies have focused on hydrological or hydraulic modeling individually, the combination of these models with GIS and other advanced analytical techniques remains underexplored. The present study aims to address these gaps by proposing a holistic and innovative approach to flood analysis. By integrating hydrological and hydraulic models with GIS analysis, this research seeks to enhance the precision of flood simulations, provide a more accurate identification of high-risk areas, and contribute to the development of more effective flood management strategies, particularly in data-scarce and sensitive watersheds. Ultimately, this research will not only improve flood prediction accuracy but also support the creation of more robust flood mitigation strategies, water resource management, and disaster planning.

TABLE 1. Geographical and Equivalent Dimensions of the Studied Watershed

Parameter	Value
Area (km²)	250.2
Perimeter (km)	277
Watershed Length (km)	75
Minimum Elevation (m)	1166
Maximum Elevation (m)	2850
Average Elevation (m)	1598
Average Slope (%)	19
Main Stream Pure Slope (%)	0.7
Main Stream Average Slope (%)	1.4
Main Stream Length (km)	7
Equivalent Rectangle Length (km)	114
Equivalent Rectangle Width (km)	21.9
Diameter of Equal-Area Circle (km)	56.5

3. RESEARCH METHODS AND TOOLS

3. 1. Characteristics of Watershed and the Studied River Section The studied section of this river spans 30 kilometers and is located in Khorramabad County, west of the city of Khorramabad. The river flows predominantly in a northeast direction until it converges with the Kashkan River. The starting point of the studied section is located 8 kilometers southwest of the city of Khorramabad. Initially, the river passes through the vicinity of Qarq Chaqa village, and at the confluence of the Khorramabad River and the Kashkan River, known as Doab Veysian, it has the following geographic coordinates:

$X = 217898$
$Y = 3710118$

The watershed area of the studied region is 250 square kilometers, with a perimeter of 277 kilometers. The Khorramabad River serves as the access route to the Khorramabad section. The river flows parallel to this route and, after merging with the Kashkan River, which approaches from the northwest (Doab Veysian), continues along the studied section under the name of the Kashkan River, ultimately flowing toward the city of Poldokhtar.

3. 2. Research Method The WetSpa model, developed by VUB University of Brussels in Belgium, is a distributed and physically-based model designed to predict the transfer of water and energy among soil, vegetation, and the atmosphere at the watershed or regional scale with daily time steps (31). This model represents the hydrological system of a watershed, encompassing components such as the atmosphere, canopy layer, stem zone, transmission zone, and saturated zone. The watershed is divided into cells distributed heterogeneously. Each cell is divided into two main sections: bare soil and vegetated soil, both of which play significant roles in maintaining water and energy balance. The calibration of the WetSpa model was carried out using observed data from local meteorological stations, streamflow measurements, and soil moisture records. The model parameters, such as infiltration rates, evapotranspiration, and soil parameters, were calibrated through an iterative process that involved comparing model outputs with observed hydrological data and adjusting the parameters to minimize the model error. The optimization process used the Nash-Sutcliffe Efficiency (NSE) index and root mean square error (RMSE) to assess model performance, with the goal of achieving the best fit between simulated and observed data. Figure 1 illustrates a schematic representation of the hydrological processes modeled by WetSpa.

The WETSPASS model is employed to estimate long-term spatial patterns of groundwater recharge, which can serve as input for regional groundwater flow models and the analysis of regional groundwater flows. This model, developed by Batelaan and De Smedt (2001) based on the WetSpa model, is shown in Figure 2. The WetSpass model examines the transfer of water and energy among soil, vegetation, and the atmosphere under quasi-steady-state conditions. As a GIS-based distributed hydrological model, WetSpass is used to estimate evapotranspiration, surface runoff, and groundwater recharge on seasonal and annual time scales.

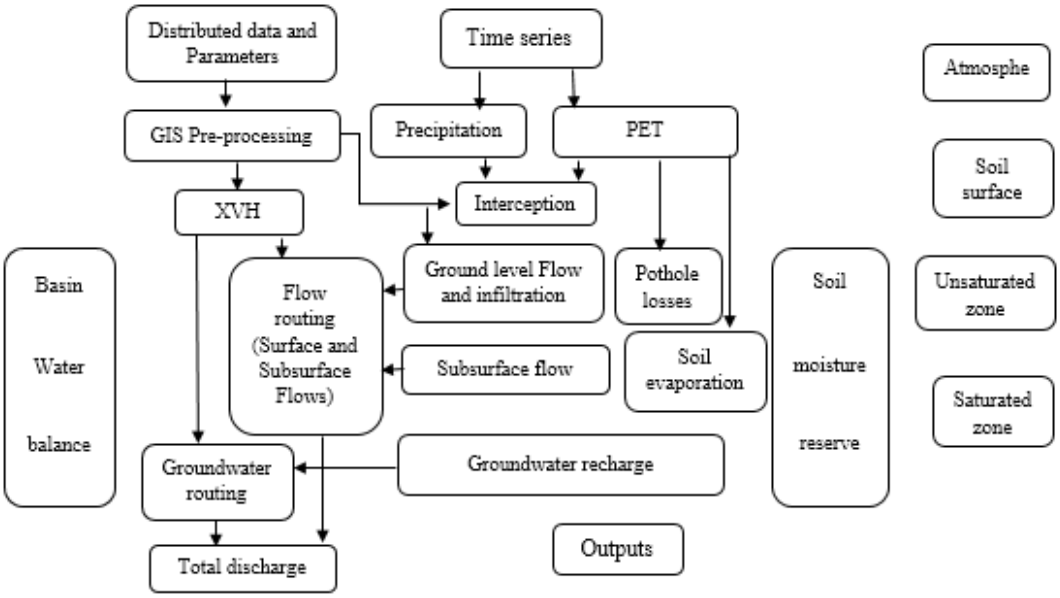

Figure 1. Main hydrological processes in the WetSpa model structure

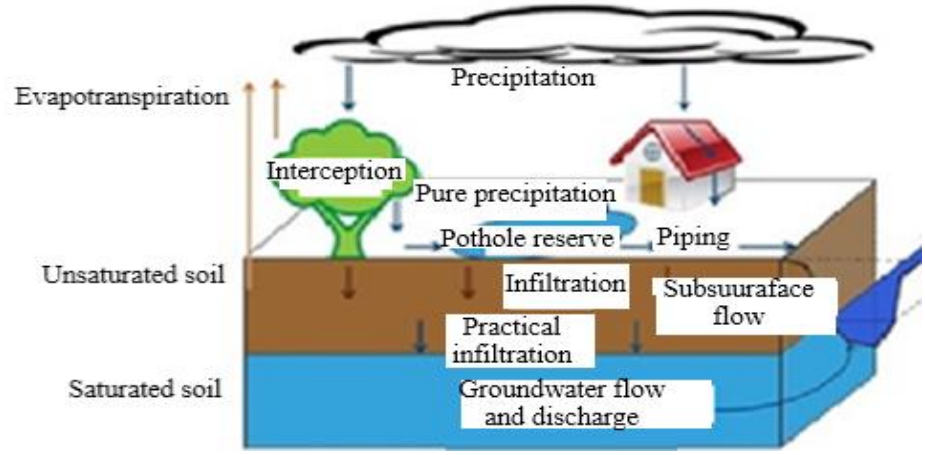

Figure 2. WetSpa model structure

The WetSpa Extension model is another GIS-based distributed hydrological model designed for flood prediction and water balance simulation at the watershed scale. This model has the capability to predict flow hydrographs at the outlet of a watershed or any other convergence point within the watershed and can simulate varying time intervals (16, 20). In addition to flood prediction, the model investigates the causes of flooding, particularly the spatial distribution of topography, land use, and soil types.

Finally, the LISFLOOD-FP hydrodynamic model is a hybrid model that simulates channel flows in one dimension and overland flows in floodplains in two dimensions. The inputs for this model are files in Ascii format that are executed in the DOS environment. The outputs of this model, also in Ascii format, include water depth at each pixel. The LISFLOOD-FP model was calibrated by adjusting parameters related to the channel flow resistance, overland flow roughness, and floodplain infiltration. The model calibration process involved using observed flood extent and water depth data, adjusting parameters through a trial-and-error method, and employing statistical measures like RMSE and the coefficient of determination (R^2) to evaluate model performance.

Regarding the performance of the WetSpa model in low-flow conditions, it has been noted that the model's accuracy decreases when simulating low-flow events. To address this limitation, model performance can be improved by refining the parameterization of infiltration

processes, particularly in areas with low runoff potential. Additionally, implementing more sophisticated land surface parameterization, such as considering the effect of soil compaction and vegetation changes on infiltration, can improve model performance during low-flow conditions. It is also recommended to integrate more local data on soil moisture and evapotranspiration to better capture the dynamics of water movement in low-flow scenarios.

4. RESEARCH FINDINGS

4. 1. Hydrological Model Calibration The calibration of the hydrological model was conducted using data from the first five years (water years 2005-2006 to 2009-2010), incorporating daily records of precipitation, temperature, and potential evapotranspiration. These datasets were extracted from a comprehensive 10-year record spanning water years 2005-2006 to 2014-2015. Additionally, daily discharge measurements from the Cham Anjir hydrometric station, located at the drainage basin outlet, were employed to compare simulated hydrographs with observed flow data during the calibration period. Calibration was performed manually using a trial-and-error approach, adjusting 11 global parameters to optimize the agreement between simulated and observed hydrographs. Both graphical and statistical comparisons were utilized to evaluate model performance. Initial parameter values were determined based on model structure, study area characteristics, and key hydrological variables. These values were subsequently refined to enhance the model's representation of observed conditions. The final calibrated parameter values are presented in Table 2, with a summary provided in Table 3. These values represent optimal estimates for simulating hydrological processes in the study area. Figure 3 illustrates a comparative analysis of the simulated and observed daily flow hydrographs, demonstrating a strong alignment between the datasets. This successful calibration validates the model's ability to replicate real-world hydrological behavior, confirming its reliability and applicability for simulating hydrological conditions in the study area.

Table 2 outlines the initial values and variation ranges of key parameters in the WetSpa model, which are essential for simulating hydrological processes. The ki parameter (sub-surface flow factor) has an initial value of 0.007, ranging from 0.1 to 10, allowing flexibility in soil permeability representation. The kg parameter (groundwater loss coefficient) starts at 0.0001, with a broad variation range (1×10^{-7} to 0.1), enabling adjustments based on local groundwater dynamics. Kss, the raw initial moisture parameter, is set at 1, ranging from 0.1 to 2, influencing soil moisture retention and runoff rates. The kep parameter (evapotranspiration correction factor) is initialized at 0.1, with a range from 0.3 to 2, allowing adaptation to vegetation and climate conditions. The Go parameter (initial groundwater reserve) is set at 10 mm, with a Gmax value reaching 5,550,000 mm, providing significant flexibility in representing groundwater storage. The To parameter (threshold degree coefficient for snowmelt) ranges from -3 to 2, accommodating diverse climatic conditions, while the ksnow coefficient (degree-day coefficient) varies from -3 to 3.2, affecting snowmelt dynamics.

The krain parameter (precipitation degree-day coefficient) ranges from 0.001 to 0.3, governing the impact of precipitation on snowmelt. The Krun parameter (surface runoff capacity) spans from 4 to 7, influencing runoff generation. Finally, the pmax parameter (maximum precipitation severity) varies from 100 mm to 5000 mm, enabling the simulation of extreme weather events. In summary, these parameters provide substantial

TABLE 2. Initial parameters and values and their ranges of variations

Sign	Parameters	Initial value	Min.	Max.
k_i	Sub-surface flow factor (-)	0.007	0.1	10
k_g	Groundwater loss coefficient (d-1)	0.0001	0.1*10-7	0.1
k_{ss}	Raw initial moisture (-)	1	0.1	2
k_{ep}	The correction factor of potential evapotranspiration (-)	0.1	0.3	2
G_o	Initial groundwater reserves (mm)	10	0	100
G_{max}	Max. initial groundwater reserve (mm)	5550000	100	10000
T_o	Threshold degree coefficient (c0)	0	-3	2
k_{snow}	Degree-day coefficient (mm c0 d-1)	0.045	-3	3.2
k_{rain}	Precipitation degree-day coefficient (mm mm c0 d-1)	0	10-3	0.3
K_{run}	Surface runoff capacity (-)	0.001	4	7
p_{max}	Max. precipitation severity (mm)	100	100	5000

flexibility, allowing the WetSpa model to be effectively calibrated for diverse environmental conditions, ranging from minimal groundwater recharge zones to regions experiencing significant precipitation and snowmelt events.

Table 3 presents the calibrated values of 11 global parameters for the WetSpa model, reflecting key hydrological processes such as infiltration, runoff, evapotranspiration, and groundwater dynamics. The ki value of 1 suggests a standard infiltration rate, allowing for effective water absorption into the soil, which is supported by the moderate kss value of 0.44, indicating substantial subsurface water storage. However, the low kg value (0.00003) implies limited groundwater recharge, suggesting that groundwater does not significantly contribute to the basin's water balance. The Go value of 140 and Gmax of 1020 highlight the capacity for groundwater storage, although recharge is slow due to the low kg coefficient. The kep value of 0.29 indicates moderate evapotranspiration, typical for areas with mixed vegetation. The low To value of 0.06 reflects initially dry soil, leading to higher runoff early in the rainfall events. With ksnow at 0.042, the snowmelt rate is low, which aligns with the similarly low krain value of 0.007, suggesting minimal runoff from rainfall. The Krun value of 3.8 suggests that runoff can become significant during intense rainfall events, and the high pmax value of 3000 enables the model to simulate extreme precipitation and flood conditions. Overall, the calibrated parameters indicate a model suited for regions where groundwater storage plays a role, but recharge is slow, and surface water dynamics, particularly runoff, are more significant during heavy rainfall events.

4. 2. WetSpa Model Validation Results The WetSpa model was validated using the global parameter values obtained during the calibration phase over a 5-year period (water years 2009–2010 to 2014–2015). The validation process involved comparing the observed daily flow hydrographs with those simulated by the model. The results of this comparison are presented in Figure 4, which offers a comprehensive overview of the model's performance during the validation phase.

The output files generated by the model provide a comprehensive view of the basin's water balance, including surface flows, subsurface flows, base flows, and total flow at each time step. These outputs are critical for assessing the model's performance and understanding the movement of water through the basin. According to the model's results, during the calibration period, 26.15% of the total precipitation is converted into runoff. This runoff is divided into surface runoff (2.37%), subsurface flow (1.61%), and groundwater discharge (base flow), which constitutes the largest portion at 22.17%.

In the validation period, the total runoff share from precipitation is slightly higher, reaching 26.42%. This slight increase suggests that the model's performance was consistent, with similar runoff dynamics observed in both

TABLE 3. Values of 11 global parameters of the WetSpa model determined in the calibration phase

Sign	Calibrated Numerical Value
ki	1
kg	0.00003
kss	0.44
kep	0.29
Go	140
Gmax	1020
To	0.06
ksnow	0.042
krain	0.007
Krun	3.8
pmax	3000

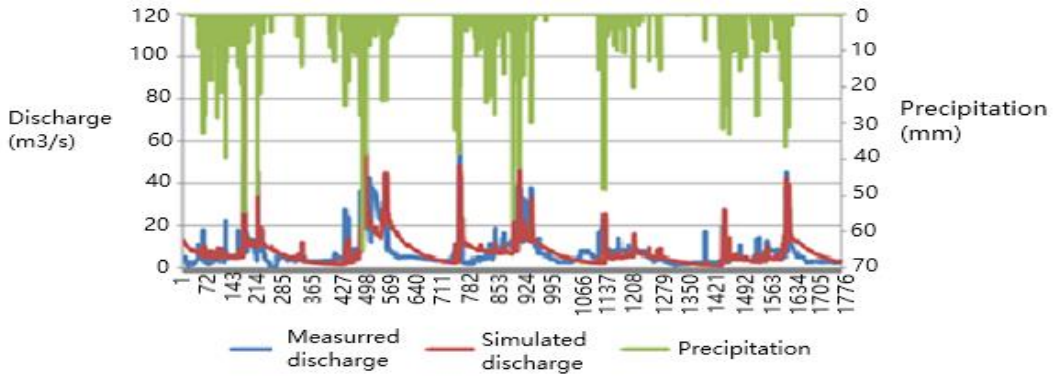

Figure 3. Comparison of the observational and simulated daily discharge hydrographs by the WetSpa model in the calibration period

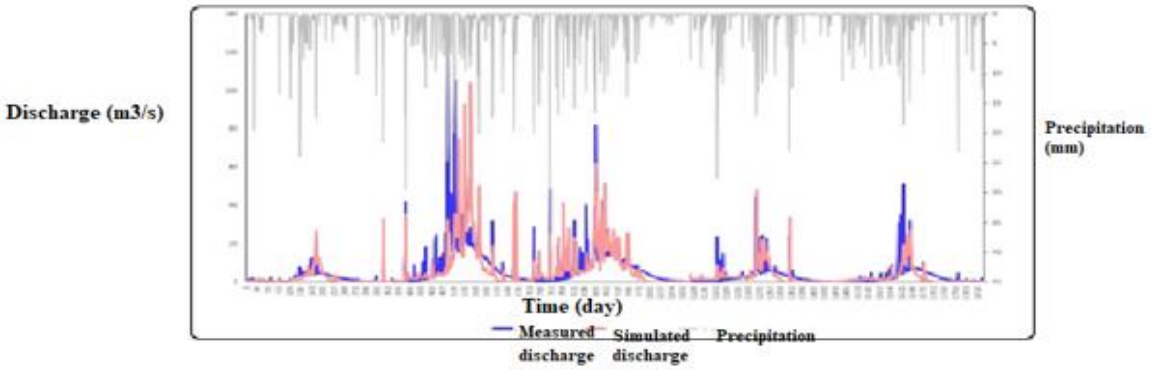

Figure 4. Comparison of the observational and simulated daily discharge hydrographs by the WetSpa model in the validation period

periods. Additionally, the model simulation results show that the ratio of evaporation to precipitation is 57.18% in the calibration period and increases to 69.20% in the validation period, indicating a higher rate of evapotranspiration during the validation phase.

Table 4 presents the water balance components calculated by the model for both the calibration and validation periods, offering a clear comparison of these key hydrological processes over time.

The variables are defined as follows: P represents the observed precipitation (mm), I denotes interception losses (mm), Ds is the change in soil moisture between the start and end of the time step (mm), F refers to infiltration losses (mm), E is evapotranspiration (mm), $PERS$ represents the main depth of infiltration outside the stem zone (mm), Ri denotes surface runoff (mm), Rg represents groundwater flow (mm), R is the total runoff (mm), and Dg refers to the change in groundwater reserves between the start and end of the time step (mm). All these components were thoroughly explained in the preceding section.

TABLE 4. Water balance components calculated by the model in the calibration period

	Sum(mm)	Precipitation (0.0)	Mean
P	2779.4	-	1.522
I	133.1	4.79	0.073
D_S	42.6	1.53	172.851
F	2067.1	74.37	1.132
E	1589.2	57.18	0.780
PERS	767.6	27.62	0.420
R_S	65.9	2.37	0.036
R_I	44.8	1.61	0.025
R_G	616.1	22.17	0.0337
R	726.9	26.15	0.398
D_G	-55.2	-1.98	108.793

4. 3. Evaluating the Efficiency of the WetSpa Model

The efficiency of the model in simulating river flows was assessed using two widely recognized performance metrics: the Nash-Sutcliffe efficiency criterion (Equation 3) and the Kling-Gupta efficiency (KGE) criterion (Equations 1 and 2). Additionally, a visual comparison of the simulated and observed hydrographs was performed to further evaluate the model's performance. The Nash-Sutcliffe efficiency (NSE) is a commonly used indicator of the model's predictive ability, with higher values reflecting better simulation accuracy. The Kling-Gupta efficiency (KGE), which incorporates key components such as correlation, bias, and variability, offers a more comprehensive assessment of model performance. Both metrics were employed to ensure a robust evaluation of the model's capability to replicate observed river flow dynamics (Tables 5 and 6).

$$KGE = 1 - \sqrt{(r-1)^2 + (\alpha-1)^2 + (\beta-1)^2}$$

$$KGE' = 1 - \sqrt{(r-1)^2 + (\alpha-1)^2 + (\gamma-1)^2}$$

$$\beta = \frac{\mu_s}{\mu_o}$$

$$\alpha = \frac{\sigma_s}{\sigma_o}$$

$$\gamma = \frac{CV_s}{CV_o} = \frac{\sigma_s/\mu_s}{\sigma_o/\mu_o}$$

Where r is the correlation coefficient between simulated and observational discharges, α the standard deviation ratio of simulated values (σ_s) to the standard deviation of observational values (σ_o), and β the mean ratio of simulated values (μ_s) to the mean observational values (μ_o). The best value for the Kling-Gupta assessment criterion is 1, which indicates full correspondence with hydrographs.

According to the modified Kling-Gupta (KGE') criterion, γ is used instead of β, which is the ratio of the coefficient of simulated value changes (CV_s) to the coefficient of observational value changes (CV_o).

$$NSE = 1 - \frac{\sum_{i=1}^{n}(O_i - P_i)^2}{\sum_{i=1}^{n}(O_i - \bar{O})^2}$$

TABLE 5. Classification of WetSpa model efficiency

Class	Excellent	Very good	Good	Weak	Very weak
Collective criterion	<85	0.7-0.8	0.7-0.55	0.55-0.4	0.4<

TABLE 6. Model assessment results based on statistical indices in calibration and validation periods

Efficiency criterion	Calibration	Validation
Nash-Sutcliffe criterion	0.53	0.48
Collective criterion	0.703	0.723
Kling-Gupta criterion	0.68	0.74

Where *NSE* is the Nash-Sutcliffe index, O_i observational discharge, P_i the predicted discharge, and $\overline{O}$ the mean observational discharges.

4. 4. LISFLOOD-FP Hydraulic Model Inputs Required for Model Implementation

4. 4. 1. Digital Model of Area Under Study The model requires a high-resolution digital elevation model (DEM) of the study area, with an appropriate cell size and accuracy to effectively capture height variations and key features of both the main channel and the floodplain. The DEM should cover a sufficiently large portion of the floodplain, including areas that are likely to be affected by flooding, to ensure a comprehensive simulation of flood dynamics and accurately represent flood risk zones. The spatial resolution of the DEM must be high enough to capture fine-scale features that influence water flow, such as floodplain depressions and embankments.

4. 4. 2. Map of the Floodplain Roughness Coefficient In areas where the floodplain does not exhibit uniform roughness, a spatially variable map of roughness coefficients must be provided. This can be achieved by assigning Manning's roughness coefficient (n) values to individual cells within a raster map, aligned with the DEM in terms of cell size and spatial resolution. This map plays a critical role in modeling the varying resistance to flow across different floodplain areas, which can significantly affect flood behavior and water distribution during high-flow events.

4. 4. 3. River Characteristics A river characteristics file is essential for defining the geometry and hydraulic properties of the river. This file includes cross-sectional profiles of the river, with the number of sections determined by changes in the river's characteristics. Each section should include specific coordinates, Manning's roughness coefficient, and the dimensions (width and depth) of the riverbed or subsurface. Accurate flow simulations depend on properly defining these river characteristics, which help to predict the flow dynamics and flood extent within the river and its floodplain.

4. 4. 4. Defining Boundary Conditions for Model Implementation Proper boundary conditions are necessary for the model's accurate implementation. The upstream boundary should be specified using an inflow hydrograph or a constant discharge value, depending on the available data. For the downstream boundary, conditions can be defined based on downstream water levels or the outflow hydrograph if a measurement station is available. In the absence of such data, boundary conditions may be inferred by calculating the normal depth and measuring the global slope of the river section. These calculations can assist in defining the downstream behavior of the flow, ensuring accurate flood predictions.

4. 5. Model Outputs

The key outputs generated by the model are as follows:

4. 5. 1. Mass Balance File This output provides a comprehensive summary of the flood event, including the extent of the flooded area, water depths, and outflow discharges in the downstream areas of the model. The mass balance file is produced for a specified time interval, which can be determined by the user, and is crucial for understanding the flow dynamics and changes over time within the study area. This file helps identify peak flood events and the associated flow characteristics, which are vital for flood risk management.

4. 5. 2. Water Depths and Water Levels for Each Pixel The model generates water depths and water level heights for each pixel within a raster network at specific time intervals defined by the user. This granular output provides detailed spatial information about water levels and depths across the entire model domain. By analyzing these outputs, researchers can pinpoint flood-prone areas and assess the dynamics of water distribution during the simulation. This information is essential for identifying regions that experience deeper or more widespread flooding.

4. 5. 3. Maximum Water Levels and Maximum Water Depths The model also outputs the maximum water level height and maximum water depth predicted for each pixel over the entire simulation period. This output is valuable for identifying areas most susceptible to extreme flooding and understanding the peak flood conditions across the entire study area. The maximum values can help in delineating flood-prone areas that may require special attention in terms of mitigation and preparedness strategies.

4. 5. 4. Channel Water Level Profile A channel water level profile is generated at specific intervals set by the user. This profile provides an in-depth view of the water levels along the river channel, helping to assess the river's behavior under different flow conditions. By analyzing this output, stakeholders can gain insights into the hydrodynamics at various locations within the channel, such as the impact of bends, obstructions, or changes in riverbed elevation on water levels during floods.

The outputs generated by the LISFLOOD-FP model provide detailed information on flood dynamics, such as water levels, water depths, and flood extents. However, integrating this data with socio-economic information is essential for effective flood risk management. Understanding the spatial distribution of flood-prone areas is key to assessing the potential social and economic impacts of flooding in vulnerable communities.

The model's ability to identify areas with varying degrees of flood susceptibility, based on different return periods, can be enhanced by incorporating socio-economic factors such as population density, land use, infrastructure, and economic activity in the floodplains. Mapping these factors in relation to the model outputs can help in identifying high-risk zones where floods may lead to significant economic losses, displacement, and disruption to critical services. Furthermore, by assessing the vulnerability of specific sectors, such as agriculture, housing, and infrastructure, policymakers can prioritize areas for flood mitigation and adaptation strategies.

Incorporating socio-economic analysis into flood risk mapping can also facilitate the development of targeted flood protection measures, including the relocation of vulnerable populations, flood-proofing infrastructure, and improving emergency response plans. The integration of these insights can make flood risk management strategies more effective by addressing both the physical and socio-economic dimensions of flooding.

4. 6. LISFLOOD-FP Hydraulic Model Validation Results In this study, the LISFLOOD-FP hydraulic model was validated using two distinct flood events with discharges of 72.64 m^3/s and 207.86 m^3/s (Table 7). These events were selected to represent moderate and extreme flooding scenarios, providing a basis for assessing the model's accuracy in predicting flood dynamics. The first event, with a discharge of 72.64 m^3/s, was chosen to evaluate the model's performance under typical flood conditions. The second event, with a higher discharge of 207.86 m^3/s, was used to test the model's ability to simulate flood behavior during more severe events. By comparing the model's simulated water levels with actual observed data from gauge stations, the validation aimed to assess the accuracy of the model's flood predictions. The results helped to identify the model's strengths in simulating flood extents and water levels, as well as any discrepancies, which may have been due to factors such as gauge accuracy or sediment accumulation. The validation process is essential to understanding the reliability of the LISFLOOD-FP model under different discharge conditions and flood intensities, and to refine its predictive capabilities for future flood risk management.

4. 7. Evaluating the Hydraulic Model in the Validation Phase based on Error Percentage Index The discrepancy observed in the model's performance, particularly for the highest discharge of 207.86 m^3/s, can be attributed to several potential factors. One primary source of error could be the accuracy of the water gauge used for validation. The gauges may be subject to technical issues such as malfunctioning sensors, which can affect the accuracy of the recorded water levels. Additionally, the accumulation of sediment at the base of the gauge is another factor that can lead to incorrect readings of the water level. This sediment buildup could obstruct the gauge's proper functioning, causing discrepancies between the actual and simulated water heights. Moreover, the quality of the input data used by the model—such as the Digital Elevation Model (DEM), roughness coefficients, and boundary conditions—could also contribute to model discrepancies. Inaccuracies in these parameters can lead to small errors in the predicted water levels and flood extents. Despite these potential sources of error, the model performed relatively well overall, demonstrating good predictive capability under most conditions.

The observations highlight the need for further refinement in both the model and the quality of the input data, particularly under extreme discharge scenarios. Improving the accuracy of these parameters could enhance the model's reliability for future flood predictions and risk assessments. Figures 5 and 6 provide visual representations of the simulated flood zones during the validation phase. These figures correspond to

TABLE 7. Model error rate of various discharges in several implementations

Discharge (m^3/s)	Water gauge height (m)	Water height in the model at the station (m)	Error rate (m)	Error percentage
50.01	2.31	2.37	0.06	2.95
72.64	2.39	2.43	0.04	1.67
207.86	3.3	3.81	0.15	15.45

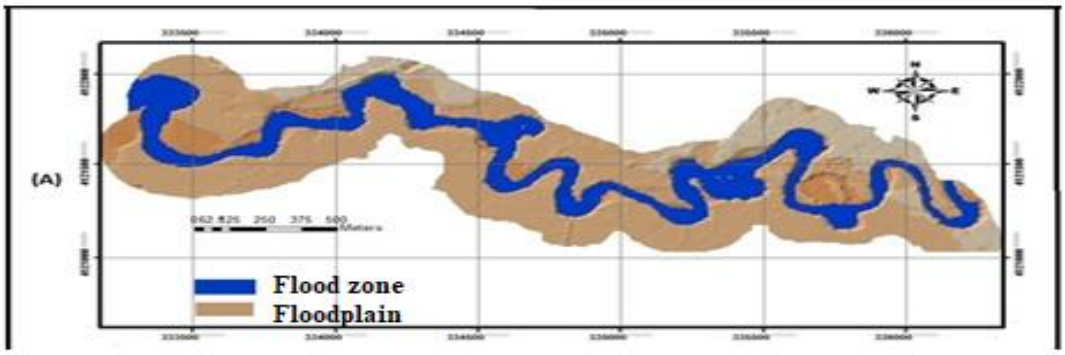

Figure 5. Flood zone simulated by the model with a discharge of 72.64 m^3/s

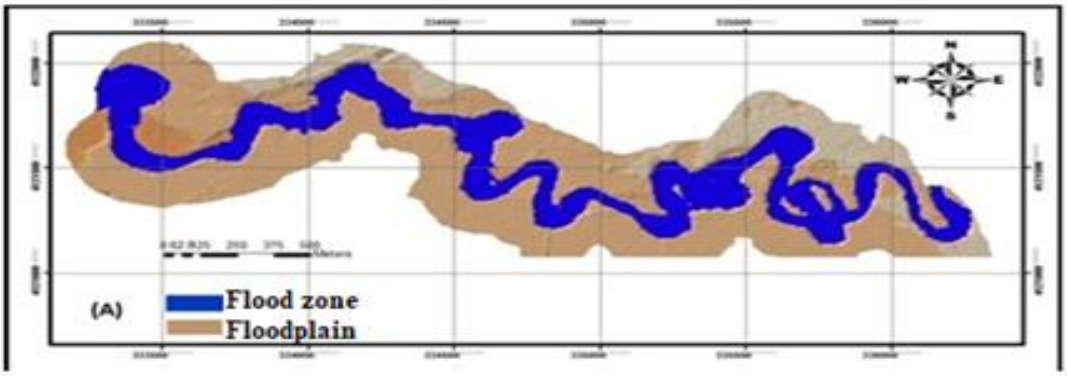

Figure 6. Flood zone simulated by the model with a discharge of 207.86 m^3/s

the two discharge events of 72.64 m^3/s and 207.86 m^3/s. The simulation results show that, in general, the flood zones align well with the areas that are expected to be prone to flooding under the given conditions. However, some minor discrepancies remain, likely due to the previously discussed factors such as sediment accumulation and input data uncertainties. By comparing the observed flood extents with the model's simulations, we can pinpoint areas where the model performed well and areas that may require further improvement. This analysis is essential for refining the model and ensuring more accurate flood risk management in future studies.

4. 8. Evaluating Integration of Two Hydrological and Hydraulic Models To assess the effectiveness of the integration between the hydrological and hydraulic models, three flood events were analyzed. These events had already been used for the calibration and validation of the hydraulic model. In the standalone application of the hydraulic model, observed hydrographs were directly used as input. However, in the integrated model approach, simulated hydrographs generated by the hydrological model were used as inputs to the hydraulic model, allowing for the simulation of the flood zones.

The integration code was applied separately for each year in which the analyzed flood events occurred. This method not only facilitated the simulation of flow hydrographs but also ensured a seamless transfer of the simulated hydrographs from the hydrological model to the hydraulic model through the integration code. This integration aimed to enhance the accuracy of flood simulations by combining the strengths of both models.

Figure 7 presents the daily flow hydrograph for a flood event with a discharge of 72.64 m^3/s, simulated using the integration code. The simulated hydrograph from the hydrological model was automatically transferred to the hydraulic model, where it was used as an upstream boundary condition for the flood simulation. This approach streamlined the process and ensured that the hydraulic model received accurate input for better flood zone predictions.

Figure 8 shows the final outlet conditions for the studied flood, illustrating the effectiveness of the integrated approach. The results demonstrate that the integration code successfully facilitated the transfer of data between the hydrological and hydraulic models, ensuring accurate simulations of the flood event.

Moreover, the findings of the LISFLOOD-FP model, particularly in identifying flood-prone areas for different return periods, offer valuable insights into areas most vulnerable to flooding. However, providing further insights into the spatial distribution of these flood-prone

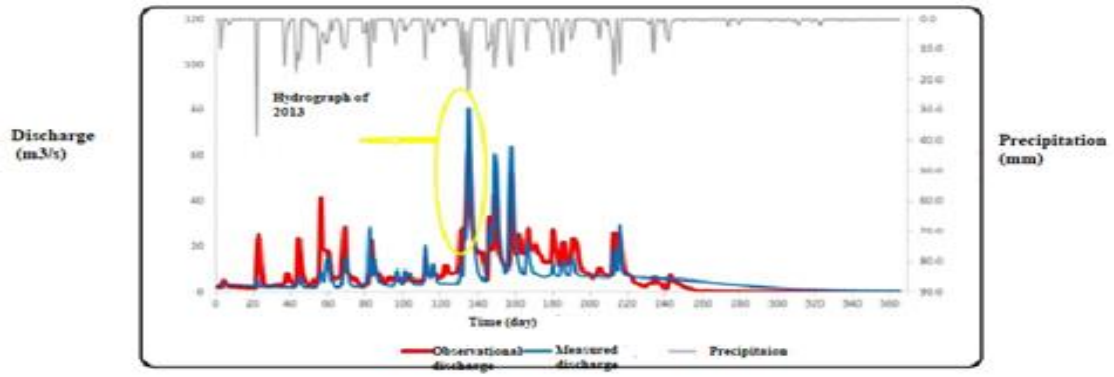

Figure 7. Observational and simulated daily flow hydrographs produced through the integration code of two models about the flood with a discharge rate of 72.64 m^3/s

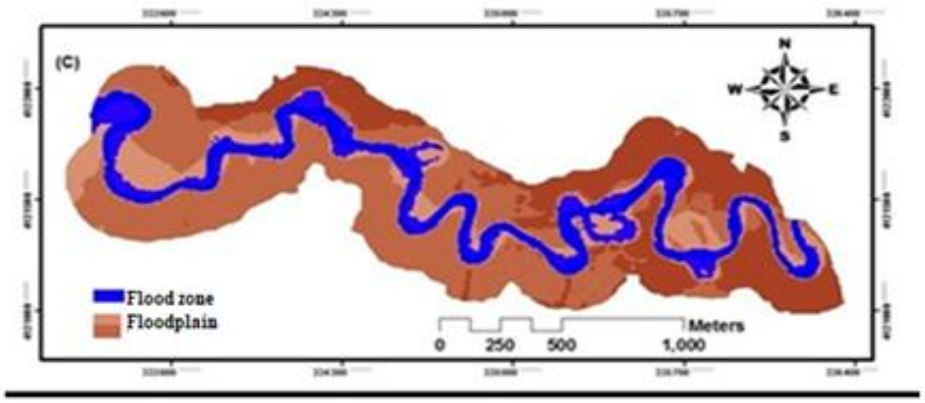

Figure 8. Flood zone with a discharge rate of 72.64 m3/s caused by a simulated inflow hydrograph

areas and their potential socio-economic impacts can significantly enhance risk management strategies. Understanding the locations and characteristics of high-risk zones can guide more targeted and effective flood mitigation efforts, helping to prioritize resources and interventions in the most vulnerable regions. The integration of both models, therefore, not only improves flood simulations but also contributes to the development of more comprehensive and informed flood risk management strategies, incorporating socio-economic factors for more holistic planning.

4. 9. Estimates of Discharges with Different Return Periods and Simulation of Flood Zones

In this study, the discharge values corresponding to return periods of 25, 50, 100, and 200 years were calculated based on a 50-year dataset that includes the maximum annual instantaneous discharges recorded at the Cham Anjir Hydrometric Station. These calculations were carried out using SMADA software, which facilitated the comparison of various statistical distributions to determine the most suitable model for the data. The chi-square goodness-of-fit tests were employed to assess the fit of the statistical distributions, ultimately leading to the selection of the Log-Pearson Type III distribution as the most appropriate model for the observed discharge data.

Following the determination of discharge estimates for the different return periods, the calibrated hydrological model was used to simulate the corresponding flood zones for each return period. The model generated spatial flood extents and water depths, providing a comprehensive view of flood behavior for the selected return periods. This simulation is essential for assessing the varying magnitudes of flood events and understanding the potential impacts of flooding on the surrounding area.

Table 6 presents the simulated results, including the maximum water depths and the total inundated areas for floods associated with different return periods. These outputs are critical for understanding the extent and severity of flood hazards under different scenarios and serve as a foundation for developing flood risk mitigation strategies. The results also provide valuable information for designing flood-control infrastructure, ensuring that the region is better prepared for future flood events.

In addition to providing detailed flood predictions, this study integrates advanced statistical methods with hydrological modeling to offer a robust framework for estimating flood risks and their spatial impacts. This integrated approach enhances the accuracy of flood predictions and contributes to more effective water resource management and disaster preparedness. By incorporating various return periods, the study also helps in understanding long-term flood risks and their implications for vulnerable areas, guiding informed decision-making and efficient resource allocation for flood risk management.

The analysis of Table 9 reveals a clear and direct relationship between discharge rates and the corresponding simulated flood zone area for return periods of 25, 50, 100, and 200 years. As the return period increases, the discharge rates also increase, from 414 m^3/s for a 25-year flood event to 620 m^3/s for a 200-year event. This increase in discharge is accompanied by a rise in the simulated flood zone area, from 539,800 m^2 for the 25-year event to 627,100 m^2 for the 200-year event. This pattern is consistent with the hydrological principles that suggest higher discharge events result in the inundation of larger areas, highlighting the escalating risk of flooding during more extreme events. Interestingly, the rate at which the flood zone area expands decreases with increasing return periods. For example, the area increases by 41,100 m^2 (7.6%) between the 25- and 50-year events, but only by 20,900 m^2 (3.4%) between the 100- and 200-year events. This diminishing rate of expansion implies that there are topographical and morphological limitations within the basin that restrict the extent of floodplain expansion despite significant increases in flow volumes. These constraints indicate that the landscape's capacity to accommodate larger flood zones becomes more limited as discharge levels rise.

The findings underscore the importance of considering both the magnitude of discharges and the spatial extent of inundation in flood risk management. The outputs generated by the calibrated model offer valuable insights into areas at higher risk of flooding, especially in extreme hydrological scenarios like the 200-year return period, which exhibits the largest zone area and discharge. This information is crucial for the development of targeted flood risk mitigation measures, land-use planning, and the design of infrastructure capable of withstanding extreme flood events. Ultimately, these results contribute to more informed decision-making in flood-prone regions, ensuring resilience and preparedness in the face of increasing flood risks.

TABLE 9. Maximum water depth and the zone area of floods with different return periods

Return period (year)	25	50	100	200
Discharge (m^3/s)	414	484	552	620
Model-simulated zone area (m^2)	539800	580900	606200	627100

5. DISCUSSION

The WetSpa model effectively simulated hydrological processes within the Khorram Abad basin, accounting for topographical, land use, and soil properties. These results align with the findings of Rad et al. (10), where the HEC-RAS model was used to assess flood-prone areas in the same region, underlining the importance of accurate flood mapping. The water balance analysis also revealed that 25.5% of the total precipitation in the basin was converted into runoff, with 2.34% as surface runoff, 1.6% as subsurface runoff, and 21.57% as groundwater discharge. However, the model performed less accurately for low-flow conditions compared to high-flow events. This discrepancy was largely due to the use of structural relationships for baseflow calculations and the limitations of the Thiessen polygon method for spatial precipitation distribution, a challenge similar to those reported in studies like Madi et al. (6) on spatial precipitation methods in Algeria.

The LISFLOOD-FP model was employed on a 7-kilometer stretch of the Khorram Abad River to simulate flood-prone areas under return periods of 25, 50, 100, and 200 years. The results indicated that as return periods increased, the flood extent also expanded, with the 200-year return period (discharge of 620 m^3/s) inundating 627,100 m^2. However, the rate of flood zone expansion diminished at higher return periods, likely due to topographical and morphological limitations within the basin. These findings corroborate the results reported by Ruidas et al. (25), who observed similar dynamics in the Gorganroud basin, emphasizing the significant role of basin-specific topography in flood modeling.

The integration of the WetSpa and LISFLOOD-FP models was implemented using Python-based code, facilitating the seamless transfer of hydrological outputs as inputs for the hydraulic model. This integration allowed for three different simulation scenarios:

1. Steady-flow simulations using constant peak discharge.
2. Unsteady-flow simulations using dynamic hydrographs over defined time steps.
3. Custom flow scenarios with user-defined time steps demonstrated excellent performance in simulating flood hydrographs and delineating flood-prone areas. This integration approach aligns with findings from Tsegaye et al. (12), where the combination of GIS and hydrological-hydraulic models proved effective in flood prediction in Florida. Moreover, the integration facilitated better management of spatial and temporal flood data, improving prediction accuracy and offering critical insights for flood management. The

study shows that integrating WetSpa and LISFLOOD-FP provides a powerful framework for simulating and managing flood events in sensitive watersheds. The models captured hydrological and hydraulic processes with accuracy, identified high-risk flood-prone areas, and contributed valuable insights for flood management strategies.

Based on the findings of this research, several recommendations can be made to enhance flood risk management and water resource planning:

Applying the Integrated Models in Other Watersheds: Extending the application of the integrated WetSpa and LISFLOOD-FP models to other basins across Iran would help identify flood-prone areas in diverse geographical contexts. However, careful consideration should be given to the hydrological and topographical characteristics of each region when transferring this modeling approach. Regions with significantly different climate, land use, or topographical features may require adjustments in model parameters, calibration, and validation methods. For instance, areas with high urbanization might require additional considerations of impervious surfaces, while regions with significant groundwater flow may need refinement in subsurface runoff simulations.

Leveraging Advanced Tools for Improved Simulation: Incorporating advanced technologies such as remote sensing and three-dimensional spatial data can further enhance simulation accuracy, particularly in regions where detailed topographical and land-use data is limited. The use of more precise elevation models and land cover datasets can help refine flood zone simulations and make predictions more reliable.

Designing Resilient Infrastructure: The results of this study can be used to inform the design of flood-resistant infrastructure, ensuring that critical infrastructure in flood-prone areas can withstand extreme events, particularly those with high return periods. Understanding the spatial extent of flooding can help in better floodplain management and design of flood barriers, drainage systems, and flood detention ponds.

Implementing Land-Use Planning: The insights gained from flood zone simulations can assist in better land-use planning, particularly in flood-prone regions, to reduce exposure and vulnerability to flood risks. By incorporating flood risk maps into urban and rural planning processes, regions can develop more sustainable practices that minimize flood risks while ensuring the continued growth of urban areas.

Impact of Climate Change: The potential impacts of climate change on flood modeling, particularly concerning changing precipitation patterns and flood intensities, should be further explored. Future studies could investigate how changing rainfall patterns and the intensity of extreme events may affect the flood-prone areas identified in this study. This would help adapt flood management strategies to future climatic conditions.

Challenges in Model Integration: A notable challenge faced during the integration of WetSpa and LISFLOOD-FP was related to computational time and the compatibility of data formats. The transfer of large datasets between the models required careful preprocessing to ensure compatibility, particularly when dealing with the spatial-temporal data outputs from the WetSpa model. Optimization of the integration process to reduce computation time is a potential area for improvement.

6. CONCLUSION

This study successfully integrated the WetSpa hydrological model and the LISFLOOD-FP hydraulic model to simulate daily flows, flood hydrographs, and flood-prone areas in the Khorram Abad drainage basin. Using a decade of meteorological data (2005–2006 to 2014–2015) as model inputs, the calibration was conducted for the first five-year period (2005–2006 to 2009–2010), while the validation relied on data from the subsequent five-year period (2009–2010 to 2014–2015). The WetSpa model demonstrated high accuracy in simulating river flows and flood hydrographs, with key performance metrics such as the Nash-Sutcliffe Efficiency (NSE) of 0.53 and the Kling-Gupta Efficiency (KGE) of 0.68. Notably, for high-flow events, the NSE reached 0.7, highlighting the model's robust capability for flood prediction.

Climate Impact on Hydrological Modeling: Future research should also consider the potential impact of climate change on hydrological modeling and flood predictions. Shifts in precipitation patterns, such as more intense rainfall or extended dry periods, could significantly alter flood dynamics and exacerbate the frequency and intensity of extreme flood events, which should be incorporated into the models for future projections.

By providing accurate flood zone simulations and offering practical recommendations, this research contributes significantly to reducing flood risks and improving water resource management in vulnerable regions like Khorram Abad. The integration of hydrological and hydraulic models has proven to be an effective tool in understanding and mitigating the impacts of flood events, fostering more informed decision-making and improved disaster preparedness.

7. REFERENCES

1. Karimi P, Safaval PA, Behzadi S, Azizi Z, Zarkash MMK, Kalashami HK. Flood risk zoning using geographical information system case study: Khorramabad Flood in April 2019. Acta hydrotechnica. 2022;35(63):89-100. https://doi.org/10.15292/acta.hydro.2022.07

2. Shayan S, Dehestani H, Hosein Zadeh MM. Geomorphologic classification of rivers in mountainous basins (case study: Khorramabad River). Quantitative Geomorphological Research. 2018;6(2):133-47.
3. Khaleghi M, Zeinivand H, Haghizadeh A. Sensitivity analysis of the spatially distributed hydrological WetSpa model parameters in estimation of daily flow in Khorramabad river. Iranian Water Researches Journal. 2016;10(4):143-8.
4. Robati M, Najafgholi P, Nikoomaram H, Vaziri BM. Zoning of Critical Hubs of Climate Change (Flood-Drought) Using the Hydrologic Engineering Center-Hydrologic Modeling System and Copula Functions Case study: Khorramabad Basin. 2024. https://doi.org/10.21203/rs.3.rs-5390435/v1
5. Pralle S. Drawing lines: FEMA and the politics of mapping flood zones. Climatic Change. 2019;152(2):227-37. https://doi.org/10.1007/s10584-018-2287-y
6. Madi H, Bedjaoui A, Elhoussaoui A, Elbakai LO, Bounaama A. Flood vulnerability mapping and risk assessment using hydraulic modeling and GIS in Tamanrasset valley watershed, Algeria. Journal of Ecological Engineering. 2023;24(7). https://doi.org/10.12911/22998993/163252
7. Di Baldassarre G, Schumann G, Bates PD, Freer JE, Beven KJ. Flood-plain mapping: a critical discussion of deterministic and probabilistic approaches. Hydrological Sciences Journal–Journal des Sciences Hydrologiques. 2010;55(3):364-76. https://doi.org/10.1080/02626661003683389
8. Ghosh A, Chatterjee U, Pal SC, Towfiqul Islam ARM, Alam E, Islam MK. Flood hazard mapping using GIS-based statistical model in vulnerable riparian regions of sub-tropical environment. Geocarto International. 2023;38(1):2285355. https://doi.org/10.1080/10106049.2023.2285355
9. Jha V, Patel J, Sawant V, Tandel Y. Flood Hazard Assessment of Water-Front Geosynthetic Reinforced Soil Wall for Dam Regulation Rule Level. International Journal of Engineering Transactions A: Basics. 2023;36(4):640-8. https://doi.org/10.5829/ije.2023.36.04a.04
10. Rad M, Vafakhah M, Gholmalifard M. Flood mapping using HEC-RAS hydraulic model in part of Khorramabad watershed. Journal of Natural Environmental Hazards. 2018;7(16):211-26. https://doi.org/10.22111/jneh.2017.3343
11. Hassas H, Azizian A, Ghasemi M. A Simple Model for determining flood hazard areas. Journal of Natural Environmental Hazards. 2020;9(25):81-100. https://doi.org/10.22111/jneh.2020.31011.1549
12. Tsegaye S, Kebedew MG, Albrecht KK, Missimer TM, Thomas S, Elshall AS. Integrated GIS-hydrologic-hydraulic modeling to assess combined flood drivers in coastal regions: a case study of Bonita Bay, Florida. Frontiers in water. 2024;6:1468354. https://doi.org/10.3389/frwa.2024. 1468354
13. Chen Y. Flood hazard zone mapping incorporating geographic information system (GIS) and multi-criteria analysis (MCA) techniques. Journal of Hydrology. 2022;612:128268. https://doi.org/10.1016/j.jhydrol.2022.128268
14. Flores AB, Collins TW, Grineski SE, Amodeo M, Porter JR, Sampson CC, et al. Federally overlooked flood risk inequities in Houston, Texas: novel insights based on dasymetric mapping and state-of-the-art flood modeling. Annals of the American Association of Geographers. 2023;113(1):240-60. https://doi.org/10.1080/24694452. 2022.2085656
15. Kastridis A, Stathis D. Evaluation of hydrological and hydraulic models applied in typical Mediterranean Ungauged watersheds using post-flash-flood measurements. Hydrology. 2020;7(1):12. https://doi.org/10.3390/hydrology7010012
16. Mudashiru RB, Sabtu N, Abustan I, Balogun W. Flood hazard mapping methods: A review. Journal of hydrology. 2021;603:126846. https://doi.org/10.1016/j.jhydrol.2021.126846
17. Ahmed I, Pan ND, Debnath J, Bhowmik M, Bhattacharjee S. Flood hazard zonation using GIS-based multi-parametric Analytical Hierarchy Process. Geosystems and Geoenvironment. 2024;3(2):100250. https://doi.org/10.1016/j.geogeo.2023.100250
18. El-Bagoury H, Gad A. Integrated hydrological modeling for watershed analysis, flood prediction, and mitigation using meteorological and morphometric data, SCS-CN, HEC-HMS/RAS, and QGIS. Water. 2024;16(2):356. https://doi.org/10.3390/w16020356
19. Javidan N, Bahremand A. Separate components of the flood flow using the distributed hydrological WetSpa model in Ziarat-Gorgan watershed. Journal of Water and Soil Conservation. 2015;22(5):233-46.
20. El-Saoud WA, Othman A. An integrated hydrological and hydraulic modelling approach for flash flood hazard assessment in eastern Makkah city, Saudi Arabia. Journal of King Saud University-Science. 2022;34(4):102045. https://doi.org/10.1016/j.jksus.2022.102045
21. Cea L, Álvarez M, Puertas J. Using integrated hydrological–hydraulic modelling and global data sources to analyse the February 2023 floods in the Umbeluzi Catchment (Mozambique). Natural Hazards and Earth System Sciences. 2024;24(1):225-43. https://doi.org/10.5194/nhess-24-225-2024
22. Hasan HH, Mohd Razali SF, Ahmad Zaki AZI, Mohamad Hamzah F. Integrated hydrological-hydraulic model for flood simulation in tropical urban catchment. Sustainability. 2019;11(23):6700. https://doi.org/10.3390/su11236700
23. Venkata Rao G, Nagireddy NR, Keesara VR, Sridhar V, Srinivasan R, Umamahesh N, et al. Real-time flood forecasting using an integrated hydrologic and hydraulic model for the Vamsadhara and Nagavali basins, Eastern India. Natural Hazards. 2024;120(7):6011-39. https://doi.org/10.1007/s11069-023-06366-3
24. Anselmo V, Galeati G, Palmieri S, Rossi U, Todini E. Flood risk assessment using an integrated hydrological and hydraulic modelling approach: a case study. Journal of hydrology. 1996;175(1-4):533-54. https://doi.org/10.1016/S0022-1694(96)80023-0
25. Ruidas D, Pal SC, Saha A, Roy P, Pande CB, Islam ARMT, et al. Flood hazard forecasting and management systems: A review of state-of-the-art modelling, management strategies and policy-practice gap. International Journal of Disaster Risk Reduction. 2024;108:104539. https://doi.org/10.1016/j.ijdrr.2024.104539
26. Fernández-Nóvoa D, González-Cao J, García-Feal O. Enhancing flood risk management: a comprehensive review on flood early warning systems with emphasis on numerical modeling. Water. 2024;16(10):1408. https://doi.org/10.3390/w16101408
27. Borga M, Anagnostou E, Blöschl G, Creutin J-D. Flash flood forecasting, warning and risk management: the HYDRATE project. Environmental Science & Policy. 2011;14(7):834-44. https://doi.org/10.1016/j.envsci.2011.05.017
28. Kumar V, Sharma KV, Caloiero T, Mehta DJ, Singh K. Comprehensive overview of flood modeling approaches: A review of recent advances. Hydrology. 2023;10(7):141. https://doi.org/10.3390/hydrology10070141
29. Al-Omari AA, Shatnawi NN, Shbeeb NI, Istrati D, Lagaros ND, Abdalla KM. Utilizing remote sensing and GIS techniques for flood hazard mapping and risk assessment. Civil Engineering Journal. 2024;10(5):1423-36. https://doi.org/10.28991/CEJ-2024-010-05-05
30. Yanfatriani E, Marzuki M, Vonnisa M, Razi P, Hapsoro CA, Ramadhan R, et al. Extreme rainfall trends and hydrometeorological disasters in tropical regions: implications for climate resilience. Emerg Sci J. 2024;8(5):1860-74. https://doi.org/10.28991/ESJ-2024-08-05-012

31. Supratman M, Kusuma MS, Cahyono M, Kuntoro AA. Flood hazard assessment due to changes in land use and cover. Civil Engineering Journal. 2024;10(12):3874. https://doi.org/10.28991/CEJ-2024-010-12-04

Persian Abstract

چکیده

هدف این مطالعه بررسی کاربرد رویکرد یکپارچه مدل‌سازی هیدرولوژیکی-هیدرولیکی برای شبیه‌سازی جریان‌های رودخانه‌ای، هیدروگراف‌های سیلاب و نواحی مستعد سیلاب در حوضه آبریز خرم‌آباد، ایران است. در این مطالعه، از مدل هیدرولوژیکی WetSpa و مدل هیدرولیکی LISFLOOD-FP برای شبیه‌سازی جریان‌های رودخانه‌ای و نواحی سیلابی استفاده شد. برای شبیه‌سازی‌ها از داده‌های هواشناسی ده‌ساله (سال‌های آبی ۲۰۰۵-۲۰۰۶ تا ۲۰۱۴-۲۰۱۵) استفاده گردید. مدل‌ها با استفاده از داده‌های پنج سال اول کالیبره شدند و داده‌های پنج سال بعدی برای اعتبارسنجی به کار رفت. مدل WetSpa برای شبیه‌سازی جریان‌های روزانه و مدل LISFLOOD-FP برای شبیه‌سازی نواحی مستعد سیلاب تحت دوره‌های برگشتی مختلف استفاده شد. مدل WetSpa توانست جریان‌های روزانه را با دقت قابل قبولی شبیه‌سازی کند و شاخص‌های عملکردی مانند کارآیی نش-ساتکلیف (NSE) معادل ۰.۵۳ و کارآیی کلینگ-گوپتا (KGE) معادل ۰.۶۸ را به‌دست آورد. برای رویدادهای جریان بالا، ضریب NSE به ۰.۷ رسید که نشان‌دهنده کارآیی مدل در پیش‌بینی سیلاب‌ها است. نتایج مدل LISFLOOD-FP نشان داد که حداکثر وسعت سیلاب برای دوره برگشتی ۲۰۰ ساله برابر با ۶۲۷,۱۰۰ متر مربع بوده است. تحلیل تعادل آب نشان داد که ۲۵.۵٪ از بارش‌ها به رواناب تبدیل شده است که شامل ۲.۳۴٪ رواناب سطحی، ۱.۶٪ رواناب زیرسطحی و ۲۱.۵۷٪ جریان آب‌های زیرزمینی می‌باشد. این مطالعه نشان می‌دهد که یکپارچگی مدل‌های هیدرولوژیکی و هیدرولیکی می‌تواند به‌طور مؤثری رفتار سیلاب‌ها را پیش‌بینی کرده و نواحی پرخطر را شبیه‌سازی کند.